A PVT Estimation for the ERTMS Train Control Systems in presence of Multiple Tracks

A. Neri [1], A.M. Vegni [1], and F. Rispoli [2]
[1] RADIOLABS, Rome Italy, {*alessandro.neri*, *annamaria.vegni*}*@radiolabs.it*
[2] Ansaldo STS , Genoa Italy, *francesco.rispoli@ansaldo-sts.com*

BIOGRAPHIES

Alessandro NERI is Full Professor in Telecommunications at the Engineering Department of the University of ROMA TRE. In 1977 he received the Doctoral Degree in Electronic Engineering from the University of Rome "Sapienza". In 1978 he joined the Research and Development Department of Contraves Italiana S.p.A. where he gained a specific expertise in the field of radar signal processing and in applied detection and estimation theory, becoming the chief of the advanced systems group. In 1987 he joined the INFOCOM Department of the University of Rome "Sapienza" as Associate Professor in Signal and Information Theory. In November 1992 he joined the Electronic Engineering Department of the University of Roma TRE as Associate Professor in Electrical Communications, and became full professor in Telecommunications in September 2001. His research activity has mainly been focused on information theory, signal theory, and signal and image processing and their applications to both telecommunications systems and remote sensing.
Since December 2008, Prof. Neri is the President of the RadioLabs Consortium, a non-profit Consortium created in 2001 to promote tight cooperation on applied research programs between universities and industries.

Anna Maria VEGNI is Assistant Professor in Telecommunications at the Department of Engineering of University of Roma Tre, Rome, Italy. She received the Ph.D. degree in Biomedical Engineering, Electromagnetics and Telecommunications from University of Roma TRE in 2010.
From May 2009 to October 2009, she was a visiting scholar in the Multimedia Communication Laboratory, at the Department of Electrical and Computer Engineering, Boston University, Boston, MA. Her research activity is focusing on vehicular networking, indoor and outdoor localization, GNSS and Visible Light Communications. Since 2011, she is in charge of Telecommunications Networks Laboratory course at Roma Tre University.

Francesco RISPOLI is responsible for the Satellite and Telecommunication projects in Ansaldo STS since 2011. Previously, he has been with Telespazio (2005-2011) as chief of the New Initiatives for strategic projectson telemedicine, emergency telecommunications, broadband internet on trains and satellite-based train control systems. By 1983 to 2005 he was with Alenia Spazio (now Thales Alenia Space) where he served various positions as responsible for R&D and institutional programs, vice president of multimedia business unit, general manager of the EuroSkyWay newco for broadband service provisioning. He has been a co-founder of the Telbios company for telemedicine services and member of the its management board. He started his carier in 1980 with Contraves Italiana S.p.A. as technical engineer in the antenna department. In 1978 he received the Doctoral Degree in Electronic Engineering fromt the Polytechnic of Turin. In 1980 he has achieved a Master in Applied Electromagnetism from the University La Sapienza in Roma.

ABSTRACT

GNSS has been recognized a strategic asset for favoring the evolution of the modern railways signaling systems that play a major role to prevent accidents due to human errors. The European ERTMS-ETCS train control system has already envisaged the utilization of GNSS for supporting the odometry function in its evolving path to provide cost-effective solutions for the low traffic lines and, more in general, for those lines which are in semi desert areas where it is imperative to limit the wayside equipment along the line. ..
The main challenge for the introduction of GNSS-based localization systems on the train signaling systems is to guarantee the same safety levels of the current systems based on wayside equipment (balyse) to estimate the exact train position and the rail where the train is travelling. This latter requirement is at least one order of magnitude more stringent respect to the determination of the train position along the track and, for that reason it requires today the support of the train driver who has to confirm in which rail the train is located. Based on these requirements and since the GNSS constellations are rapidly evolving towards a redundant and resilient global infrastructure, we have developed a novel multi-constellation PVT algorithm for train localization

determination, specifically designed to handle the case of multiple track scenarios. This solution is driven by the requirements of the ERTMS-ETCS train control system and compliant with the SIL-4 safety requirements of CENELEC railways norms *i.e.*, Tolerable Hazard Rate (THR), $10^{-9} \leq \text{THR} \leq 10^{-8}$.

To meet the SIL 4 requirements, we adopted a GNSS architecture comprising of a dedicated integrity monitoring and augmentation network, as well as the use of multi-constellation receivers.

The PVT algorithm estimates the train location by explicitly accounting for the fact that the train is constrained to lie on a railway track. Basically, exploiting this constraint allows to estimate train location even when only two satellites are in view. Effective reduction in the number of required satellites to make a fix, when track constraint is applied, depends on the track-satellite geometry. In essence, satellites aligned along the track give more information than those at the cross-over. By implementing this technique, the satellites in excess are taken into consideration for the elaboration of the PVT only to achieve the desired accuracy, integrity and availability specifically for the rail application.

In this paper, we address the problem of PVT estimation of the train in presence of multiple tracks. This can be formulated as a combination of hypothesis testing (*i.e.*, which is the current track where the train lies on, or, better, which is the probability of a train lying on a given track?) and parameter estimation (i.e. given a track, which is the curvilinear abscissa of the train receiver?).

A detailed description of the overall PVT process is given. The performance of the track detector versus inter-track distance, observation time duration, signal-to-noise ratio and observables (*i.e.*, pseudoranges and carrier phase) are discussed. Then, the impact of satellite failures on the PVT error magnitude and track detection is exploited. Finally, the assessment of the performance is also provided by means of simulation results making use of both synthetic data (Monte Carlo simulations), and measures recorded on a railway test bed environment as a part of the 3InSat project co-funded by the European Space Agency (ESA) in the framework of the ARTES 20 programme.

I. INTRODUCTION

Modern signaling systems play a major role to provide automatic train protection (ATP) to prevent accidents due to human errors. The deployment of the European radio-based signaling train control system, ERTMS-ETCS, mainly for the high speed lines is contributing to a *de-facto* global standard in terms of both interoperability among different national systems and for the highest safety level achieved. On the other hands the development of the GALILEO system in Europe has also contributed to the study of safety of life applications for rail [1].

A synergy between GALILEO and ERTMS-ETCS is now becoming a reality since the signature of the new Memorandum of Understanding (MoU) for the evolution of the ERTMS-ETCS that has envisaged the adoption of the GNSS to improve its competitiveness in the global market and for the local and regional lines. However, the main challenge in the adoption of GNSS-based Location Determination Systems (LDS) is constituted by the information integrity imposed by the safety requirements of the railways specifications that is generally different and more stringent of the integrity requirement specified by the aeronautical scenario.

In the ERTMS-ETCS system, the Hazardous Failure Rate (HFR) during 1 hour of operation shall be less than 10^{-9} for SIL-4 compliant systems. It implies that the probability that the magnitude of the error of the position provided by the LDS shall not exceed the Alarm Level (*AL*), that is the maximum allowed error, while this event is not detected by the Integrity Monitoring algorithm (e.g. protection Level $PL<AL$), has to be in principle less than $2\cdot10^{-13}$. However the ETCS platform can mitigate some risks relevant to the detection of the virtual balyses that represent the points along the line where the PVT is estimated.

To reach the challenging SIL 4 target, we propose a LDS architecture, which considers (*i*) a multi-constellation capability to manage both accuracy, availability and redundancy, (*ii*) the deployment of a Track Area Augmentation and Integrity Monitoring Network with very high availability, and (*iii*) an independent on-board capability to further mitigate GNSS errors, and autonomously assess the GNSS location integrity, when augmentation data are unavailable.

The Augmentation Network includes a Ranging & Autonomous Integrity Monitoring (RAIM) reference stations, co-located with selected communications base stations for the purpose of integrity monitoring, accuracy improvement of satellite-based position, and for providing correction to mobile receivers. Each reference station has an LDS Safety Server, to elaborate the corrections and to detect systematic satellite faults. Finally, to enhance the systematic satellite fault detection capabilities, the outputs from reference stations are jointly processed by a Track Area LDS Safety (TALS) server.

Railways applications are referred as safety-related systems, a sub case of the well known safety-of-life GNSS application and they requires a higher performance especially in terms of availability, continuity, integrity and accuracy. Conventional, stand-alone, GPS systems are unable to provide the positioning information with an error bounded by a protection level compliant with the safety requirements of railways applications. On the other hands, recent developments of GNSS prove to be inspiring for safety-of-life applications: for instance, modernized GNSS signals are broadcast with increased power and enhanced characteristics for multipath mitigation, while the presence of multiple constellations may potentially increase the overall availability along a rail line.

To meet the SIL-4 requirements, we believe that a GNSS system characterized by a dedicated integrity monitoring and augmentation network and by the use of multi-constellation receivers offers in perspective an higher degree of flexibility. More in detail, in our system, the train is equipped with the GNSS Location Determination System On-Board Unit (LDS OBU), which provides the PVT estimate to the existing train odometry system. Each GNSS LDS OBU is equipped with (*i*) two GNSS receivers, (*ii*) a local processor performing the PVT estimation starting from local measures, (*iii*) a track Data Base and the augmentation data received from a Track Area LDS Safety (TALS) server, and (*iv*) a communication module.

The PVT algorithm estimates the train location by explicitly accounting for the fact that the train is constrained to lie on a railway track. Basically, by exploiting this constraint it is possible to estimate the train location even when only two satellites are in view. Effective reduction in the number of required satellites to make a fix, when track constraint is applied, depends on the track-satellite geometry. In essence, satellites aligned along the track give more information than those at the cross-over. Satellites in excess can then be employed either to increase accuracy or to increase integrity and availability. In [2], we presented a SIL-4 solution for PVT train estimation, for the single-track scenarios. However, in multiple-track scenarios, the ERTMS-ETCS also requires track discrimination. This is far more challenging than PVT estimation alone, due to the fact that inter-track separation is rather smaller compared to the confidence error allowed for localizing the train along the same track. As a matter of fact, the cross-track protection level (*i.e.*, 1.5 m) is one order of magnitude lower than the along track protection level (*i.e.*, 15 m). These aspects concerning the adoption of GNSS for railway signalling and train control for the migration from aviation risk to hazard rate and safety integrity level, and the dependability assessment of Satellite Based Augmentation System for Signalling and Train Control are discussed in detail in [3], [4]. While, respectively, in [6] and [7] the Galileo Integrity Concept and the GBAS Integrity for non-aviation users are provided.

Here we present a novel algorithm that combines single track PVT estimate with track detection. In particular, for each candidate track, we estimate the curvilinear abscissa of the receiver by means of a Weighted Least Square Estimator (WLSE), assuming that the corresponding hypothesis is true. Then, we compute the measurement residuals conditioned to each hypothesis and from them the *a posteriori* probability of each track.

All those a posteriori probabilities can be combined in a generalized log-likelihood ratio tests to detect the current track. In fact, assuming that the hypotheses are uniformly distributed, the Bayesian (optimal) track detection rule selects the hypothesis corresponding to the largest of them. However, to reach track error probabilities compatible with the SIL 4 requirement, multiple observations have to be combined. Since the generalized log-likelihood ratio magnitudes provide information about the reliability of each hypothesis, their values are compared to thresholds to verify that enough information has been acquired before a decision on which track the train is lying on is transmitted to the ATP processor.

For each track, the conditional PVT estimate is computed by solving a set of non-linear equations relating the observables (*e.g.* pseudoranges and carrier phases) to the receiver curvilinear abscissa and clock offset, by means of an iterative Weighted Least Square Error (WLSE) procedure, accounting for the different statistics of the equivalent measurement noise, due to both satellite elevation and signal characteristics specific of each constellation.

This paper is organized as follows. We briefly recall the LDS architecture used in our model, as previously described in [2]. The LDS algorithm for PVT train estimation is then illustrated, first for the case of single track estimation, and then for the multi-track case. Simulation results are then shown in order to assess the effectiveness of the PVT technique. Finally, conclusions are drawn at the end of the paper.

II. LDS ARCHITECTURE

In order to fulfill the basic SIL 4 requirement four basic criteria have been considered in designing the architecture of the GNSS based train LDS system:

1) exploitation of multiple constellations, in order to increase both system integrity and availability;
2) use of wide area augmentation systems like WAAS and EGNOS, where available, for accuracy and precision increase, as well as integrity monitoring. These networks should be updated in future in order to meet specific railway needs and assure the interoperability with different localization systems;
3) deployment of a dedicated Augmentation and Integrity Monitoring Network, co-located with a set of TLC base stations, in regions not served by augmentation networks fulfilling the railway requirements;
4) independent on-board capability to mitigate GNSS errors, and autonomously assess the GNSS location integrity.

Considering that satellite ephemerides and clock errors, as well as anomalous propagation conditions in ionosphere and troposphere represent the most relevant sources of hazard for the LDS, adoption of a Ranging and Integrity Monitoring network plays a major role in preventing that any Hazardous Misleading Information may be provided by the On Board LDS unit, without a timely warning.

In fact, processing of satellite signals received at known locations allows to estimating the error sources, which affect train positioning, as well as to detecting eventual GNSS, and more in general Signal In Space (SIS) faults. Compared to actual EGNOS, supporting SIL 4 compliant railway applications may require the deployment of spatially denser RIM stations. On the other hand, to increase SIS availability, the wireless network employed for train signaling is also used for distributing augmentation and integrity information to the LDS OBUs. Thus, since integrity should be assessed for any visible constellation, the RIMs shall adopt multi-constellation receivers. As a matter of fact, the Dilution of Precision (DoP) associated to the estimation the current train location strictly depends on the number of visible satellites, as well as on their line of sight geometry. Use of a multi-constellation receiver reduces the need of higher number of visible satellites that results highly redundant. As a consequence, the DoP decreases.

The on-board LDS comprises a dual-path GPS receiver integrated with a SIL-4 processor board. The LDS on-board component is a self-contained unit that connects to the ATP, the antennas, and the locomotive power supply.

Each reference station has an LDS Safety Server based on the same SIL-4 system, as the mobile LDS On Board units, but configured to provide correction services and detect systemic satellite faults.

In order to enhance the systemic satellite fault detection capabilities, as well as to detect eventual faults of the regional LDS Safety Servers, their outputs are jointly processed by a Track Area LDS Safety (TALS) server. Such architecture allows improving the correction function of classical differential GPS systems and mitigating the risk of failure relevant to the GPS reference stations.

As depicted in Figure 1 the LDS system architecture is structured in a modular way. The overall system comprises three sub-systems:

1) RIM Reference Stations (RS);
2) TALS Server;
3) On Board Unit (OBU).

In particular, the set of RSs with RIM functionalities, distributed along the railway, and TALS server constitutes the Augmented and Integrity Monitoring Network (AIMN).

The Augmentation and Integrity Monitoring Network (AIMN) is based on two sub-systems *i.e.*, (*i*) the RIM Stations, and (*ii*) TALS server. It provides the differential corrections to be applied to the GNSS LDS OBU for compensating for the effects produced by satellite ephemerides and clock offset errors, as well as the variation in the propagation delay introduced by ionosphere and troposphere, and in addition AIMN monitors SIS integrity.

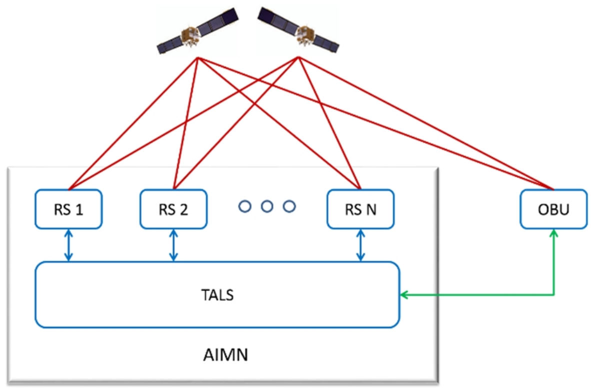

Figure 1. LDS overall architecture. Legend: Signal In Space (*red lines*), RS to TALS application protocol (*blue lines*), and TALS to OBU application protocol (*green line*).

Finally, the GNSS LDS OBU provides PVT estimates, as well as an indication of their accuracy. Each RIM RS is equipped with:

i. independent GNSS receiving chains;
ii. a local processing facility, denoted in the following as LDS Safety Server;
iii. a communication module.

The pseudoranges provided by each RIM station are jointly processed by a central processing facility, named in the following as TALS server, that (*i*) monitors the integrity of the received SISs, then evaluating the health status of each satellite, and providing an estimate of the error sources statistics, and (*ii*) estimate the differential corrections to be applied by each GNSS LDS OBU.

Table 1. RIM RS, TALS, and OBU Functionalities.

RIM RS	***TALS***	***OBU***
Signal-In-Space Receive and Decode	TALS Server RIM RS Data Exchange	Signal-In-Space Receive and Decode
Pseudorange Residual Computation	GNSS Navigation Data Quality Monitoring	Pseudorange Residual Computation
GNSS Measurement Consistency Check	Differential Corrections Computation	GNSS Measurement Consistency Check
Pseudorange Residual Combination	SIS Fault Detection & Integrity Assessment	PVT Estimation
RIM RS TALS Server Data	TALS Server GNSS LDS OBU Data Exchange	Autonomous Integrity Monitoring

Exchange		

Finally, The GNSS LDS OBU will provide the PVT estimate and the confidence interval to the existing localization system.

Each GNSS LDS OBU is equipped with (*i*) independent GNSS receivers, (*ii*) a local processor performing the PVT estimation starting from local measures, the Track DB and augmentation data received from the TALS server, and (*iii*) a track database (Track DB).

III. SINGLE TRACK PVT ESTIMATION

In this section, we present the weighted least square PVT estimation for train positioning, under the constraint of lying on a single railway track.

From a mathematical point of view, track constraint can be imposed by observing that the train location at a given time t is completely determined by the knowledge of its distance from one head end, *i.e.*, by the curvilinear abscissas defined on the geo referenced railway track. Let $s(t)$ be the curvilinear abscissa of a train reference point, like the center of the antenna of the GNSS receiver, when the GNSS pseudoranges at time are is measured. Without loss of generality, we refer here the train reference point to the ECEF frame. Thus subscripts 1, 2, 3 will identify the corresponding coordinates. Incidentally, we observe, that since we are measuring ranges (or pseudo-ranges) and the Euclidean L2 norm is invariant with respect to changes of orthonormal basis, the measurement equations can be equivalently expressed in any orthonormal basis.

Then, observing that the Cartesian coordinates) of that point are described by the parametric equations

$$\mathbf{X}^{Train}(t) = \mathbf{X}^{Train}\{s(t)\} = \\ = \begin{bmatrix} x_1^{Train}[s(t)] & x_2^{Train}[s(t)] & x_3^{Train}[s(t)] \end{bmatrix}^T \quad (1)$$

the pseudoranges measured by the GNSS receiver can be directly expressed in term of the unknown curvilinear abscissa, also denote in the following as the *train mileage*.

In fact, the pseudo-range $\rho_i(k)$ of the i-th satellite measured by the OBU GNSS receiver can be written as follows

$$\rho_i(k) = \left\| \mathbf{X}_i^{Sat}\left[T_i^{Sat}(k)\right] - \mathbf{X}^{Train}\left[s(T_i^{Train}(k))\right] \right\| + \\ + c\Delta\tau_i^{ion}(k) + c\Delta\tau_i^{trop}(k) + c\delta t^{Train}(k) + \\ + n_i^{Train}(k) - c\delta t_i^{Sat}(k) \quad (2)$$

where

- $T_i^{Sat}(k)$ is the time instant on which the signal of the k-th epoch is transmitted from the i-th satellite;
- $\mathbf{X}_i^{Sat}\left[T_i^{Sat}(k)\right]$ is the coordinate vector of the i-th satellite at time $T_i^{Sat}(k)$;
- $\Delta\tau_i^{ion}(k)$ is the ionospheric incremental delay along the path from the i-th satellite to the GNSS receiver for the k-th epoch w.r.t. the neutral atmosphere;
- $\Delta\tau_i^{trop}(k)$ is the tropospheric incremental delay along the path from the i-th satellite to the GNSS receiver for the k-th epoch w.r.t. the neutral atmosphere;
- $\delta t_i^{Sat}(k)$ is the offset of the i-th satellite clock for the k-th epoch;
- $T_i^{Train}(k)$ is the time instant of reception by the OBU GNSS receiver of the signal of the k-th epoch transmitted by the i-th satellite;
- $\delta t^{Train}(k)$ is the OBU receiver clock offset;
- $n_i^{Train}(k)$ is the error of the time of arrival estimation algorithm generated by multipath, GNSS receiver thermal noise and eventual radio frequency interference.

For sake of compactness in the following we drop temporal dependence on the epoch index.

A similar equation can be written for carrier phase tracking.

Let:

- $\hat{\mathbf{X}}_i^{Sat}\left[T_i^{Sat}\right]$ be the coordinate vector of the i-th satellite estimated on the basis of the broadcasted navigation data and eventual SBAS data where available;
- $\Delta\hat{\rho}_i^{Sat}\left[T_i^{Sat}\right]$ be the component of the differential correction related to the ephemerides error of the i-th satellite provided by the TALS server (although TALS server may provide an overall correction, it can always be modeled as the sum of individual corrections);
- $\varepsilon_{\Delta\hat{\rho}_i^{Sat}}\left[T_i^{Sat}\right]$ be the residual estimation error of the differential corrections of the ephemerides error of the i-th satellite provided by the TALS server;

so that we can write:

$$\left\| \mathbf{X}_i^{Sat}\left[T_i^{Sat}(k)\right] - \mathbf{X}^{Train}\left[s\left(T_i^{Train}(k)\right)\right] \right\| = \\ = \left\| \hat{\mathbf{X}}_i^{Sat}\left[T_i^{Sat}(k)\right] - \mathbf{X}^{Train}\left[s\left(T_i^{Train}(k)\right)\right] \right\| + \\ + \Delta\hat{\rho}_i^{Sat}\left[T_i^{Sat}\right] + \varepsilon_{\Delta\hat{\rho}_i^{Sat}}\left[T_i^{Sat}\right] \quad (3)$$

In addition, let:

- $\Delta\hat{\tau}_i^{ion}(k)$ be the component of the differential correction related to estimated ionospheric incremental delay along the path from the i-th satellite to the GNSS receiver for the k-th epoch w.r.t. the neutral atmosphere;
- $\Delta\hat{\tau}_i^{trop}(k)$ be the component of the differential correction related to estimated tropospheric incremental delay along the path from the i-th satellite to the GNSS receiver for the k-th epoch w.r.t. the neutral atmosphere;
- $\varepsilon_{\hat{\tau}_i^{ion}}$ be the estimation error of the ionospheric

incremental delay along the path from the i-th satellite to the GNSS receiver for the k-th epoch w.r.t. the neutral atmosphere;

- $\varepsilon_{\hat{\tau}_i^{trop}}$ be the estimation error of the tropospheric incremental delay along the path from the i-th satellite to the GNSS receiver for the k-th epoch w.r.t. the neutral atmosphere;
- $n_i^{Train}(k)$ be the measurement error of the OBU GNSS receiver for the k-th epoch

$$n_i^{Train}(k) = n_i^{Train,Mp}(k) + n_i^{Train,Rx}(k) + n_i^{Train,RFI} \quad (4)$$

where

 - $n_i^{Train,Mp}(k)$ is the measurement error due to multipaths from the i-th satellite to the GNSS receiver for the k-th epoch;
 - $n_i^{Train,Rx}(k)$ is the measurement error due to the thermal plus the internal receiver noise affecting the signal received from the i-th satellite for the k-th epoch;
 - $n_i^{Train,RFI}$ is the measurement error due to the radio frequency interference affecting the signal received from the i-th satellite for the k-th epoch
 - .

- $\delta\hat{t}_i^{Sat}$ be the component of the differential correction related to estimated offset of the i-th satellite clock provided by the TALS server;
- $\varepsilon_{\delta\hat{t}_i^{Sat}}$ be estimation error of the offset of the i-th satellite clock for the k-th epoch, so that we can write

$$\delta t_i^{Sat} = \delta\hat{t}_i^{Sat} + \varepsilon_{\delta\hat{t}_i^{Sat}}. \quad (5)$$

Therefore, for the pseudorange expression, we can write

$$\begin{aligned}\rho_i(k) = {} & \left\| \hat{\mathbf{X}}_i^{Sat}\left[T_i^{Sat}\right] - \mathbf{X}^{Train}\left[s(T_i^{Train})\right] \right\| + \\ & + \Delta\hat{\rho}_i^{Sat}\left[T_i^{Sat}\right] + c\varepsilon_{\Delta\hat{\rho}_i^{Sat}}\left[T_i^{Sat}\right] + \\ & + c\Delta\hat{\tau}_i^{ion} + c\Delta\hat{\tau}_i^{trop} - c\delta\hat{t}_i^{Sat} + c\delta t^{Train} + \\ & + c\varepsilon_{\Delta\hat{\tau}_i^{ion}} + c\varepsilon_{\Delta\hat{\tau}_i^{trop}} - c\varepsilon_{\delta\hat{t}_i^{Sat}} + n_i^{Train} \quad , \end{aligned} \quad (6)$$

Denoting with $\delta\hat{\rho}_i^{Diff}$ the overall differential correction provided by the Augmentation and Integrity Monitoring Network as

$$\delta\hat{\rho}_i^{Diff} = \Delta\hat{\rho}_i^{Sat} + c\Delta\hat{\tau}_i^{ion} + c\Delta\hat{\tau}_i^{trop} - c\delta\hat{t}_i^{Sat}, \quad (7)$$

we finally obtain

$$\begin{aligned}\rho_i - \delta\hat{\rho}_i^{Diff} = {} & \left\| \hat{\mathbf{X}}_i^{Sat}\left[T_i^{Sat}\right] - \mathbf{X}^{Train}\left[s(T_i^{Train})\right] \right\| + c\delta t^{Train} + \\ & + n_i, \end{aligned} \quad (8)$$

with

$$n_i = c\varepsilon_{\Delta\hat{\rho}_i^{Sat}} + c\varepsilon_{\Delta\hat{\tau}_i^{ion}} + c\varepsilon_{\Delta\hat{\tau}_i^{trop}} - c\varepsilon_{\delta\hat{t}_i^{Sat}} + n_i^{Train}. \quad (9)$$

The pseudo-range equation system can be solved by an iterative procedure based on the first order Taylor's series expansion around an initial train curvilinear abscissa estimate $\bar{s}$. Notice that the initial estimate of the curvilinear abscissa is obtained by first computing the receiver location without track constraint and selecting as initial point for the iteration the position of the virtual reference station that is nearest to the train position estimated at the previous step.

Let us denote with $\tilde{\rho}_i$ the i-th pseudorange corresponding to the site with mileage equal to $\bar{s}$, i.e.,

$$\tilde{\rho}_i = \left\| \hat{\mathbf{X}}_i^{Sat}\left[T_i^{Sat}\right] - \mathbf{X}^{Train}\left[\bar{s}\right] \right\|, \quad (10)$$

so that

$$\begin{aligned}& \rho_i - \delta\hat{\rho}_i^{Diff} - \tilde{\rho}_i - c\delta t^{Train} - n_i = \\ & = \left\| \hat{\mathbf{X}}_i^{Sat}\left[T_i^{Sat}\right] - \mathbf{X}^{Train}\left[s(T_i^{Train})\right] \right\| - \left\| \hat{\mathbf{X}}_i^{Sat}\left[T_i^{Sat}\right] - \mathbf{X}^{Train}\left[\bar{s}\right] \right\| \end{aligned} \quad (11)$$

Then, denoting with

$$\Delta s = s\left(T_i^{Train}\right) - \bar{s}, \quad (12)$$

we expand the term

$$\chi = \left\| \hat{\mathbf{X}}_i^{Sat}\left[T_i^{Sat}\right] - \mathbf{X}^{Train}\left[s(T_i^{Train})\right] \right\| \quad (13)$$

in Taylor's series w.r.t. s with initial point $\bar{s}$, then obtaining

$$\begin{aligned}\chi = {} & \left\| \hat{\mathbf{X}}_i^{Sat}\left[T_i^{Sat}\right] - \mathbf{X}^{Train}\left[\bar{s}\right] \right\| \\ & + \left[\frac{\partial\rho_i}{\partial x_1^{Train}}\frac{\partial x_1^{Train}}{\partial s} + \frac{\partial\rho_i}{\partial x_2^{Train}}\frac{\partial x_2^{Train}}{\partial s} + \frac{\partial\rho_i}{\partial x_3^{Train}}\frac{\partial x_3^{Train}}{\partial s} \right]_{s=\bar{s}} \Delta s + \\ & + n_i^{Taylor} \end{aligned} \quad (14)$$

where n_i^{Taylor} accounts for the expansion truncation. Then, we finally obtain:

$$\begin{aligned}& \rho_i - \delta\hat{\rho}_i^{Diff} - \tilde{\rho}_i = \\ & = \left[\frac{\partial\rho_i}{\partial x_1^{Train}}\frac{\partial x_1^{Train}}{\partial s} + \frac{\partial\rho_i}{\partial x_2^{Train}}\frac{\partial x_2^{Train}}{\partial s} + \frac{\partial\rho_i}{\partial x_3^{Train}}\frac{\partial x_3^{Train}}{\partial s} \right]_{s=\bar{s}} \Delta s + \\ & \quad + c\delta t^{Train} + n_i + n_i^{Taylor}, \end{aligned} \quad (15)$$

with $i = 1, \ldots, N_{Sat}$, and N_{Sat} as the number of visible satellites.

Now, denoting with $\Delta\rho_i$ the differential reduced pseudo range

$$\Delta\rho_i = \rho_i - \delta\hat{\rho}_i^{Diff} - \tilde{\rho}_i, \quad (16)$$

the corresponding N_{Sat} scalar linear equations can be written in compact matrix notation as follows

$$\Delta\rho = \mathbf{HDz} + \mathbf{\nu}, \quad (17)$$

where $\mathbf{z}$ is the array

$$\mathbf{z} = \begin{bmatrix} \Delta s \\ c\delta t^{Train} \end{bmatrix}, \quad (18)$$

D is the matrix with elements given by the directional cosines of the tangent to the railway track at the point with mileage equal to $\bar{s}$:

$$\mathbf{D} = \begin{bmatrix} \left[\frac{\partial x_1^{Train}}{\partial s}\right]_{s=\bar{s}} & 0 \\ \left[\frac{\partial x_2^{Train}}{\partial s}\right]_{s=\bar{s}} & 0 \\ \left[\frac{\partial x_3^{Train}}{\partial s}\right]_{s=\bar{s}} & 0 \\ 0 & 1 \end{bmatrix}, \quad (19)$$

H is the classical $N_{Sat} \times 4$ observation matrix:

$$\mathbf{H} = \begin{bmatrix} \mathbf{P} & \mathbf{1}_{N_{Sat}} \end{bmatrix}, \quad (20)$$

where **P** is the $N_{Sat} \times 3$ Jacobian matrix of the pseudo-ranges,

$$\mathbf{P} = \left[\frac{\partial \boldsymbol{\rho}}{\partial \mathbf{X}^{Train}}\right]_{\mathbf{X}^{Train}=\mathbf{X}^{Train}[\bar{s}]}, \quad (21)$$

whose elements are given by the directional cosines of the satellite lines of sight:

$$P_{ij} = \left[\frac{\partial \tilde{\rho}_i}{\partial x_j^{Train}}\right]_{\mathbf{X}^{Train}=\mathbf{X}^{Train}[\bar{s}]} = -\frac{x_{i,j}^{Sat} - x_j^{Train}[\bar{s}]}{\left\|\mathbf{X}_i^{Sat} - \mathbf{X}^{Train}[\bar{s}]\right\|}, \quad (22)$$

with $j = 1, 2, 3$, and $\mathbf{1}_{N_{Sat}}$ is the $N_{Sat} \times 1$ vector:

$$\mathbf{1}_{N_{Sat}} = \begin{bmatrix} 1 \\ 1 \\ \vdots \\ 1 \end{bmatrix}, \quad (23)$$

and, finally,

$$\nu_i = n_i + n_i^{Taylor} =$$
$$= c\varepsilon_{\Delta\hat{\rho}_i^{Sat}} + c\varepsilon_{\Delta\hat{\tau}_i^{ion}} + c\varepsilon_{\Delta\hat{\tau}_i^{trop}} - c\varepsilon_{\delta\hat{t}_i^{Sat}} + n_i^{Train} + n_i^{Taylor} \quad (24)$$

represents the equivalent observation noise (with $i = 1, 2, \ldots, N_{Sat}$).

A similar set of linear equations can be written when pseudoranges derived from carrier phase tracking are employed.

The set of linear equations (17) may be solved w.r.t. the curvilinear abscissa, and the receiver clock offset by means of a weighted least square, numerical procedure that accounts for the different statistics of the error of the time of arrival estimates related to satellites of different constellations.

We remark that, with respect to ordinary least square solution, it accounts for different characteristics of errors related to satellites of different generations and dependence of receiver noise from satellite elevation, as in case of tropospheric incremental delay and multipath components.

Therefore the described algorithm can be directly employed when a mix of satellites from different constellations are used, as far as eventual differences in their timing references are pre-compensated. Nevertheless it can be also applied to subsets of the visible satellites belonging to the same constellation.

Recently, particle filters have been proposed in place of extended Kalman filters to solve the pseudorange nonlinear equations. Nevertheless, their computational complexity qualifies them as not mature for high integrity receivers.

At each iteration, the weighted least square estimate $\overline{\mathbf{Z}}$ is computed as

$$\hat{\mathbf{z}} = \mathbf{K}\Delta\boldsymbol{\rho} \quad (25)$$

where **K** is the gain matrix

$$\mathbf{K} = \left(\mathbf{D}^T\mathbf{H}^T\mathbf{R}_\nu^{-1}\mathbf{H}\mathbf{D}\right)^{-1}\mathbf{D}^T\mathbf{H}^T\mathbf{R}_\nu^{-1} \quad (26)$$

In addition, the variance of the estimate of the curvilinear abscissa s computes as follows

$$\sigma_s^2 = \left[\mathbf{R}_{\Delta\hat{\mathbf{z}}}\right]_{1,1} = \left[\left(\mathbf{D}^T\mathbf{H}^T\mathbf{R}_\nu^{-1}\mathbf{H}\mathbf{D}\right)^{-1}\right]_{1,1}. \quad (27)$$

Finally we set $\bar{s} \doteq \bar{s} + \Delta\hat{z}_{11}$ and the whole procedure is reiterated until a convergence criterion is met (e.g., magnitude of the incremental mileage correction below a predefined value).

IV. MULTI TRACK WEIGHTED LEAST SQUARE PVT ESTIMATION

When the railway consists of multiple tracks, the single track PVT estimate is combined with track detection.

Let us assume that the train can be located along one of M tracks and let denote with H_k the hypothesis corresponding to the k-th track.

Then, denoting with $\Lambda_k(\boldsymbol{\rho})$ the generalized likelihood ratio given by the condition probability density function of the observations $\boldsymbol{\rho}$ with respect to the k-th hypothesis H_k divided by any arbitrary function that does not depend on H_k:

$$\Lambda_k(\boldsymbol{\rho}) = \frac{p_{\mathrm{P}/H_k}(\boldsymbol{\rho}/H_k)}{w(\boldsymbol{\rho})}, \quad (28)$$

and assuming that the hypotheses are uniformly distributed, the Bayesian (optimal) track detection rule selects the hypothesis corresponding the largest $\Lambda_k(\boldsymbol{\rho})$, or equivalently to the largest $\ln\Lambda_k(\boldsymbol{\rho})$.

On the other hand, as illustrated in the previous paragraph, $\boldsymbol{\rho}$ is a function of the unknown train curvilinear abscissa and receiver clock offset, and of the observation noise $\boldsymbol{\nu}$. Thus for each hypothesis, i.e., for each track, we have

$$\boldsymbol{\rho} = \tilde{\boldsymbol{\rho}}_{H_k} + \delta\hat{\boldsymbol{\rho}}_{H_k}^{Diff} + \mathbf{H}_{H_k}\mathbf{D}_{H_k}\mathbf{z}_{H_k} + \boldsymbol{\nu}. \quad (29)$$

Now, as in [8], we proceed by first estimating $\mathbf{z}_k$ under the hypothesis that H_k is true, and then we use these estimates in a likelihood ratio test, as if they were correct. Thus for each hypothesis the generalized log-likelihood functional $\ln \tilde{\Lambda}_k(\boldsymbol{\rho})$ is computed, where

$$\ln \tilde{\Lambda}_k(\boldsymbol{\rho}) = \underset{\mathbf{z}_{H_k}}{Max} \ln \frac{p_{\mathrm{P}/H_k}(\boldsymbol{\rho}/\hat{\mathbf{z}}_{H_k})}{w(\boldsymbol{\rho})} . \quad (30)$$

Then the hypothesis corresponding to the largest generalized log-likelihood functional is selected.
Since conditioned to the k-th hypothesis, $\boldsymbol{\rho}$ is a Gaussian random variable with (conditional) expectation

$$E\left\{\boldsymbol{\rho}/\hat{\mathbf{z}}_{H_k}, H_k\right\} = \tilde{\boldsymbol{\rho}}_{H_k} + \delta\hat{\boldsymbol{\rho}}_{H_k}^{Diff} + \mathbf{H}_{H_k}\mathbf{D}_{H_k}\hat{\mathbf{z}}_{H_k} \quad (31)$$

and covariance matrix

$$Cov\left\{\boldsymbol{\rho}/\hat{\mathbf{z}}_{H_k}, H_k\right\} = \mathbf{R}_{\mathbf{v}} \quad (32)$$

then, by selecting

$$w(\boldsymbol{\rho}) = \frac{1}{\left[(2\pi)^{N_{sat}} \det\left(\mathbf{R}_v\right)\right]}, \quad (33)$$

we have

$$\ln \tilde{\Lambda}_k(\boldsymbol{\rho}) = \underset{\mathbf{z}_{H_k}}{Max} \ln \frac{p_{\mathbf{P}/H_k}(\boldsymbol{\rho}/\hat{\mathbf{z}}_{H_k})}{\left[(2\pi)^{N_{sat}} \det\left(\mathbf{R}_{\mathbf{v}}\right)\right]^{-1/2}} =$$

$$= \underset{\mathbf{z}_{H_k}}{Max}\left\{-\frac{1}{2}\left(\boldsymbol{\rho} - \tilde{\boldsymbol{\rho}}_{H_k} - \delta\hat{\boldsymbol{\rho}}_{H_k}^{Diff} - \mathbf{H}_{H_k}\mathbf{D}_{H_k}\hat{\mathbf{z}}_{H_k}\right)^T \mathbf{R}_{\mathbf{v}}^{-1}\right.$$

$$\left.\left(\boldsymbol{\rho} - \tilde{\boldsymbol{\rho}}_{H_k} - \delta\hat{\boldsymbol{\rho}}_{H_k}^{Diff} - \mathbf{H}_{H_k}\mathbf{D}_{H_k}\hat{\mathbf{z}}_{H_k}\right)\right\} . \quad (34)$$

Incidentally we observe that the estimate of $\mathbf{z}_k$ employed in track detection is the one for which

$$\hat{\mathbf{z}}_{H_k} = Arg\left\{\underset{\mathbf{z}_{H_k}}{Min}\left[\left(\Delta\boldsymbol{\rho}_{H_k} - \mathbf{H}_{H_k}\mathbf{D}_{H_k}\mathbf{z}_{H_k}\right)^T \mathbf{R}_{\mathbf{v}}^{-1}\right.\right.$$

$$\left.\left.\left(\Delta\boldsymbol{\rho}_{H_k} - \mathbf{H}_{H_k}\mathbf{D}_{H_k}\mathbf{z}_{H_k}\right)\right]\right\}. \quad (35)$$

Thus, denoting with

- $\Delta\breve{\boldsymbol{\rho}}_{H_k}$ the differential reduced pseudo range at the final iteration when the train is assumed to be located along the k-th track;
- $\breve{\mathbf{H}}_{H_k}\breve{\mathbf{D}}_{H_k}$ the observation matrix at the final iteration when the train is assumed to be located along the k-th track;
- $\hat{\mathbf{z}}_{H_k}$ the estimate of train curvilinear abscissa and receiver clock offset vector at the final iteration when the train is assumed to be located along the k-th track;
- $\hat{\mathbf{v}}_{H_k}$ the vector of the residuals corresponding to the k-th hypothesis,

$$\hat{\mathbf{v}}_{H_k} = \Delta\breve{\boldsymbol{\rho}}_{H_k} - \breve{\mathbf{H}}_{H_k}\breve{\mathbf{D}}_{H_k}\hat{\mathbf{z}}_{H_k} \quad (36)$$

- $\mathbf{C}_{\mathbf{v}}$ the matrix

$$\mathbf{C}_{\mathbf{v}} = diag\begin{bmatrix} \frac{1}{\sigma_{v_1}} & \frac{1}{\sigma_{v_1}} & \cdots & \frac{1}{\sigma_{v_{NSat}}} \end{bmatrix} \quad (37)$$

  so that $\mathbf{R}_{\mathbf{v}}^{-1} = \mathbf{C}_{\mathbf{v}}^T\mathbf{C}_{\mathbf{v}}$
- $\boldsymbol{\zeta}_{H_k} = \mathbf{C}_v\hat{\mathbf{v}}_{H_k}$ the normalized vector of the residuals corresponding to the k-th hypothesis,

and with $\left\|\boldsymbol{\zeta}_{H_k}\right\|^2$ the weighted squared L^2 norm

$$\left\|\boldsymbol{\zeta}_{H_k}\right\|^2 = \hat{\mathbf{v}}_{H_k}^T\mathbf{R}_{\mathbf{v}}^{-1}\hat{\mathbf{v}}_{H_k}, \quad (38)$$

we have

$$\ln \tilde{\Lambda}_k(\boldsymbol{\rho}) = -\frac{1}{2}\left\|\boldsymbol{\zeta}_{H_k}\right\|^2 \quad (39)$$

Therefore the Bayesian detector will select the track with the smallest weighted squared L^2 norm $\left\|\boldsymbol{\zeta}_{H_k}\right\|^2$.
In addition the posterior probability of each hypothesis is approximated as follows:

$$\mathrm{Prob}\{H_k\} = \frac{\exp\left(-\frac{1}{2}\left\|\boldsymbol{\zeta}_{H_k}\right\|^2\right)}{\sum_m \exp\left(-\frac{1}{2}\left\|\boldsymbol{\zeta}_{Hm}\right\|^2\right)}. \quad (40)$$

V. PERFORMANCE ASSESSMENT

In presence of multiple tracks, in addition to the probability that the mileage error will exceed the Alert Limit and no timely warning is provided, the relevant figure of merit for the computation of the probability of providing an hazardous misleading information is constituted by the track error probability, i.e. the probability of declaring that a train is on a wrong track. Denoting with P_e the track error probability and with P_{e_i} the conditional error probability conditioned to the vent that the i-th hypothesis is true, and assuming the a priori the M hypotheses are uniformly distributed we have

$$P_e = \sum_{i=1}^{M}\frac{1}{M}P_{e_i} \quad (41)$$

Here, for sake of compactness of the mathematical model, let us examine the case of parallel tracks without split and merge. The more general case is beyond the scope of this paper. Nevertheless, the general results can be obtained by extending the results reported here, with the aid of a Markovian model.
For the computation of P_{e_i} we observe that two different situations have to be considered: either all the remaining tracks fall on the same side of the "true" track (corresponding to i=1 and i=M) or the remaining tracks fall on both sides of the "true" track corresponding to $1<i<M$).
Based on the results of the previous paragraph, and denoting with ζ_{H_k/H_i} the normalized vector of the residuals corresponding to the k-th hypothesis when the i-th hypothesis is the true one, we will have a track error as

soon as there exists at least one hypothesis, let say the h-th one for which the normalized squared L^2 norm satisfies the condition

$$\left\| \zeta_{H_h/H_i} \right\|^2 < \left\| \zeta_{H_i/H_i} \right\|^2, \quad h \neq i \tag{42}$$

Since the PVT estimation procedure operates on a linearized system, in order to compute the statistics of ζ_{H_k} conditioned to the Hypothesis H_i, let us denote with $\hat{s}_i^{nf}$ the estimate of the train mileage for the i-th track in absence of receiver noise and multipath (noise-free case), under the condition that the i-th hypothesis is true. In addition

Let us denote with $\mathbf{b}_{i,k}$ the offset of the k-th track with respect the i-th one. Then as demonstrated in Appendix A, the conditional probability of selecting one of the other tracks when the i-th track is the true one, can be written as follows:

$$P_{e_i} = \begin{cases} \frac{1}{2} erfc\left\{ \frac{\left\| \mathbf{\Gamma}_i \mathbf{b}_{2,1} \right\|}{2\sqrt{2}} \right\} & i=1 \\ \frac{1}{2} erfc\left\{ \frac{\left\| \mathbf{\Gamma}_i \mathbf{b}_{i-1,i} \right\|}{2\sqrt{2}} \right\} + \frac{1}{2} erfc\left\{ \frac{\left\| \mathbf{\Gamma}_i \mathbf{b}_{i+1,i} \right\|}{2\sqrt{2}} \right\} & 1 < i < M \\ \frac{1}{2} erfc\left\{ \frac{\left\| \mathbf{\Gamma}_i \mathbf{b}_{M-1,M} \right\|}{2\sqrt{2}} \right\} & i = M \end{cases} \tag{43}$$

where

$$\mathbf{\Gamma}_i = \mathbf{C}_v (\mathbf{I} - \mathbf{HK}) \mathbf{P}_i . \tag{44}$$

Let us now specify the above results for the case of M equispaced coplanar parallel tracks. Let $\mathbf{e}_\perp$ the unit vector orthogonal to the track tangent and lying on the tracks' plane, al let Δb be the offset between to adjacent tracks, so that

$$\mathbf{b}_{k,i} = (k-i)\mathbf{b}_0 = (k-i)\Delta b \mathbf{e}_\perp . \tag{45}$$

Considering that in this case we have M-2 tracks (to $1<i<M$) for which the remaining tracks fall on both sides of the "true" track while we have two tracks (corresponding to i=1 and i=M) for which the remaining tracks fall on the same side of the "true" track, for the track error probability we have:

$$P_e = \left(1 - \frac{1}{M}\right) erfc\left\{ \frac{\left\| \mathbf{\Gamma}_i \mathbf{e}_\perp \right\|}{2\sqrt{2}} \Delta b \right\} . \tag{46}$$

As expected, the track error probability decreases with the track separation.

This expression applies to both code pseudorange based and carrier phase tracking track discrimination. In fact, for each satellite the projection of inter track distance on its line of sight is normalized with respect to the pseudorange equivalent noise standard deviation (see Eqs. (37) and (44)). Thus the difference in achievable performance with stand alone and differential receivers making use of C/A code pseudoranges and/or carrier phase tracking based pesudoranges, strictly depends on the different error budgets associated to the related receivers.

As illustrated in the next section devoted to the experimental results, for the Olbia-Cagliari railway values in the range [0.75, 2.1] can be expected for the quantity $\left\| \mathbf{\Gamma}_i \mathbf{e}_\perp \right\|$ in presence of 2 parallel tracks with an offset of 1.5 m and a pseudo range receiver equivalent noise variance of 1 m^2, that can be considered typical for differential GPS receivers making use of the A/C code.

This in turn implies that the corresponding worst case track error probability will be about 0.29.

On the other, the achievable equivalent pseudorange noise standard deviation when real time tracking of the carrier phase is employed (i.e. when the receiver operates in RTK mode) can be at least one orders of magnitude smaller than the one associated to the A/C code.

This in turn implies that for the case at hand the worst case track error probability drops to 10^{-8}.

To further illustrate the difference among the equivalent pseudorange noises affecting code and carrier phase based pseudoranges, in Figure 2 a detail of the train receiver locations estimated without imposing the track constraint for both, code tracking Differential GNSS, and RTK mode, using GPS and GLONASS satellites, recorded during the measurement campaign along the Roma-Salerno railway (see next section for further details) are shown.

Difference in magnitude of the cross-track error component between code and carrier phase estimates is rather evident. We further observe that selecting the track nearest to the unconstrained estimate represents just a suboptimal solution.

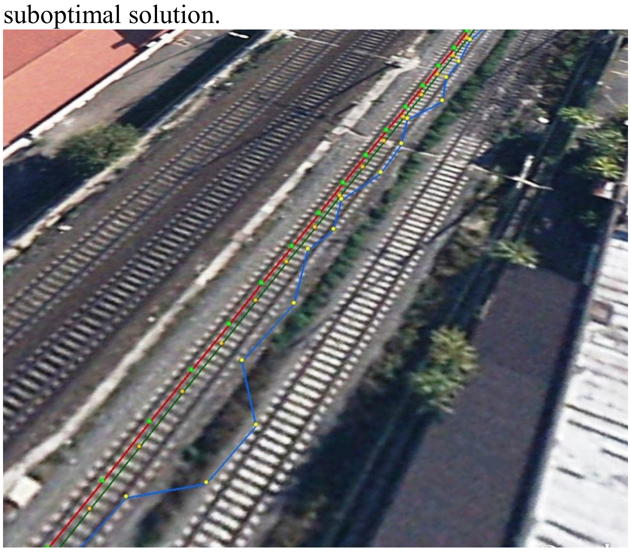

Figure 2. Detail of the Roma-Salerno measurement campaign: RTK unconstrained estimate (green-line) and code based Differential GNSS (blue line) versus ground truth (red line).

In both cases, to improve the performance multiple independent measures at different epochs can be used. In this case, two approaches can be applied.

In the first case the overall generalized likelihood ratio is computed. Thus for N_O independent observations we have

$$\mathrm{Prob}\{H_k\} = \frac{\exp\left(-\frac{1}{2}\sum_{h=1}^{N_O}\left\|\boldsymbol{\zeta}_{H_k}(t_h)\right\|^2\right)}{\sum_m \exp\left(-\frac{1}{2}\sum_{h=1}^{N_O}\left\|\boldsymbol{\zeta}_{H_m}(t_h)\right\|^2\right)}. \qquad (47)$$

Performance can then be evaluated as straightforward extension of the single epoch track detection. Thus by introducing the partitioned vector

$$\boldsymbol{\beta}_{k,i} = \begin{bmatrix} \boldsymbol{\Gamma}_i(t_1)\mathbf{b}_{k,i}(t_1) \\ \boldsymbol{\Gamma}_i(t_2)\mathbf{b}_{k,i}(t_2) \\ \vdots \\ \boldsymbol{\Gamma}_i(t_{N_O})\mathbf{b}_{k,i}(t_{N_O}) \end{bmatrix}, \qquad (48)$$

we can write

$$P_{e_i}^{(N_o)} = \begin{cases} \frac{1}{2}erfc\left\{\frac{\left\|\boldsymbol{\beta}_{2,1}\right\|}{2\sqrt{2}}\right\} & i=1 \\ \frac{1}{2}erfc\left\{\frac{\left\|\boldsymbol{\beta}_{\mathrm{i-1,i}}\right\|}{2\sqrt{2}}\right\} + \frac{1}{2}erfc\left\{\frac{\left\|\boldsymbol{\beta}_{\mathrm{i+1,i}}\right\|}{2\sqrt{2}}\right\} & 1<i<M \\ \frac{1}{2}erfc\left\{\frac{\left\|\boldsymbol{\beta}_{M-1,M}\right\|}{2\sqrt{2}}\right\} & i=M \end{cases} \qquad (49)$$

As particular case, we observe that for equispaced coplanar tracks, and a slowly moving train (ideally a still train) the track error probability, when N_O epochs are employed, is

$$P_e^{(N_O,I)} = \left(1-\frac{1}{M}\right)erfc\left\{\frac{\left\|\boldsymbol{\Gamma}_i\mathbf{e}_\perp\right\|}{2\sqrt{2}}\sqrt{N_O}\Delta b\right\} (50)$$

In the second case, a rank order statistics test can be employed. For instance, we decide that the train is lying on the i-th track if at least for k_O out of N_O epochs the norm $\left\|\boldsymbol{\zeta}_{H_i}(t_h)\right\|^2$ is the smallest one. Although the solution devised in the first case is the optimal one in presence of Gaussian observation noise, use of rank order statistics provides a more robust outlier resilience and, therefore, it appears as a better candidate when strong multipath has to be faced.

Concerning performance, for equispaced coplanar tracks, and a slowly moving train, the single epoch track error probability can be considered constant during the observation interval, and for the evaluation of the overall track error probability the Bernoulli distribution applies. Thus we can write

$$P_e^{(N_O,II)} = 1 - \sum_{h=k_O}^{N_0}\binom{N_O}{h}\left(1-P_e\right)^h P_e^{N_O-h}. \qquad (51)$$

Considering track discrimination integrity, we observer that undetected satellite faults and/or incremental ionospheric and tropospheric delays not fully compensated by the augmentation system, may potentially affect the track error probability.

The loss in track error probability can be assessed using Eq. (69) of Appendix A.

However, to reduce the impact on integrity we force in the track discrimination algorithm the use of the same gain and the same observation matrix for each hypothesis, so that due the isotropic behavior of the pdf of $\boldsymbol{\zeta}_{H_i}$ Eq.(46) and Eq. (50) are still valid.

VI. EXPERIMENTAL RESULTS

To verify the impact of the satellite geometry on the track discrimination capabilities of the proposed algorithm, the track error probabilities have been computed for a reference case of a set of 24 trains travelling along a 350 km route, from Cagliari to Olbia (Italy), at a nominal speed of 80 km/hour, and leaving from Cagliari every our, with the aid of the 3InSat GNSS simulator [5]. In the performed evaluation the masked areas as tunnel and bridges have been neglected.

The map of the selected railway is reported in Figure 3.

In Figure 4 and Figure 5 the quantity $\left\|\boldsymbol{\Gamma}_i\mathbf{b}_0\right\| / \left\|\mathbf{b}_0\right\| = \left\|\mathbf{C}_\mathrm{v}(\mathbf{I}-\mathbf{HK})\mathbf{P}_i\mathbf{e}_\perp\right\|$ versus the train mileage, when code tracking is used and the GPS-EGNOS receiver equivalent noise variance is 1 m^2, is is reported for GPS constellation based PVT and joint GPS-GLONASS-EGNOS PVT estimates. GLONASS receiver equivalent noise is scaled w.r.t. to the GPS one based on the characteristics of waveforms and modulations of the two constellations. GLONASS augmentation data availability for EGNOS services has been assumed.

Based on the reported results it appears that when the GPS alone is employed, for that particular railway, the key performance indicator $\left\|\boldsymbol{\Gamma}_i\mathbf{b}_0\right\| / \left\|\mathbf{b}_0\right\|$ presents a lower bound of about 0.75, while when both GPS and GLONASS satellites are employed the over bound is about 1.45.

Figure 3. The Olbia-Cagliari railway

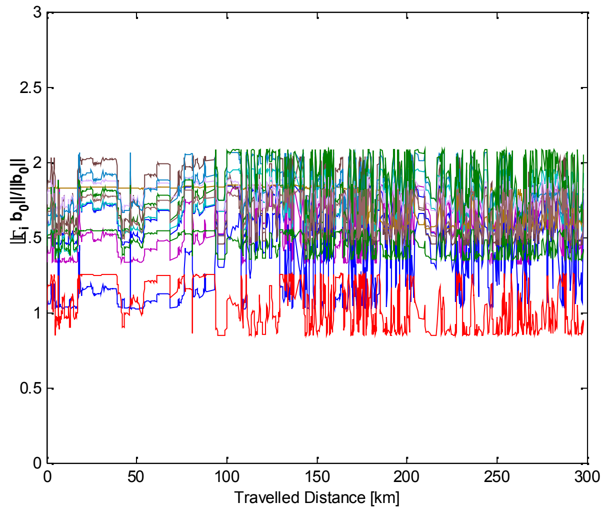

Figure 4. Normalized key performance indicator $\left\|\boldsymbol{\Gamma}_i \mathbf{b}_0\right\| / \left\|\mathbf{b}_0\right\| = \left\|\mathbf{C}_v(\mathbf{I}-\mathbf{HK})\mathbf{P}_i \mathbf{e}_{\perp}\right\|$ versus train mileage – GPS only.

By means of Eq.(46) and Eq. (50), it can be easily verified that in presence of 2 parallel tracks with an offset of 1.5 m, to achieve a track error probability of 10^{-11} (two orders of magnitude lower than the HMI probability of 10^{-9} in 1 hour) we need about 130 epochs when the GPS alone is employed, and about 40 epochs when both constellations GPS and GLONASS are used.

To further verify the effectiveness of the GNSS based train LDS, a measurement campaign has been performed, in the framework of the 3InSat research project, by means of a diagnostic train CARONTE (CAR ON TEchnology) provided by the Italian Railway Operator RFI (Rete Ferroviaria Italiana). The train was moving along the Rome-Salerno route (around 300 km), in a sunny day, with minimal impact of local atmospheric disturbances (see Figure 6).

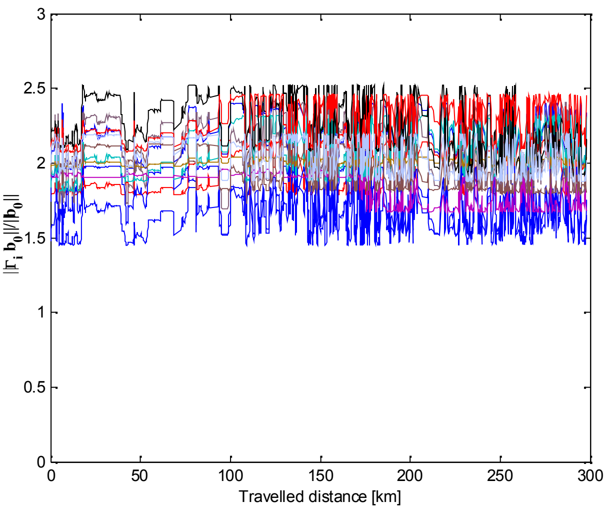

Figure 5. Normalized key performance indicator $\left\|\boldsymbol{\Gamma}_i \mathbf{b}_0\right\| / \left\|\mathbf{b}_0\right\| = \left\|\mathbf{C}_v(\mathbf{I}-\mathbf{HK})\mathbf{P}_i \mathbf{e}_{\perp}\right\|$ versus train mileage – GPS – GLONASS code tracking.

The train was equipped with a 3G Internet connection based on multi mobile carriers on the Italian territory (*i.e.*, Democrito system). For the test, an antenna with magnetic mount (Tallysmann TW2410), of diameter less than 10 cm, able to receive GPS, GLONASS and SBAS (EGNOS) signals of single frequency L1 and having an LNA gain equal to 25 dB min. on the band from 1575.42-1606 MHz has been installed on the roof of the train.

Figure 6.. Rome-Cassino railway (part of Rome-Salerno railway).

The antenna was positioned above the cab 1 of the train, with an offset of about 40 centimeters on the carriage's left side with respect to the central axis of the train; the TW2410 was connected via an RF cable of 5 m length to an evaluation-kit with on-board low-cost, single frequency, code and carrier phase, multi-constellation GNSS receiver (*i.e.*, GPS, GLONASS, GALILEO, COMPASS, SBAS).

As reference, collected data were also processed with RTKLIB software supporting both absolute positioning algorithms (*i.e.*, stand-alone) and precise positioning algorithms (*i.e.*, Differential GNSS Real Time Kinematic, and Precise Point Positioning), with corrections received from the ItalPos network in RTK Nearest mode (1 sec correction-rate).

.

Figure 7. RFI CARONTE diagnostics train.

The recorded data set has been post processed, to evaluate the performance of the multiple track detector, in case of

two parallel tracks with an inter-track offset of 2 m. Since the measurement campaign has been made at an early stage of the 3InSat project, the psudoranges provided by the ItalPos network have been employed as input to the augmentation and integrity monitoring network, in place of those provided by RIMs' receivers.
Moreover, for similar reason the track data base has been built on the basis of the train location estimated by post processing the carrier phase with a Differential GNSS Real Time Kinematic algorithm. This in turn implies that the reported evaluation is also affected by track data base inaccuracies, mostly due to multipath.

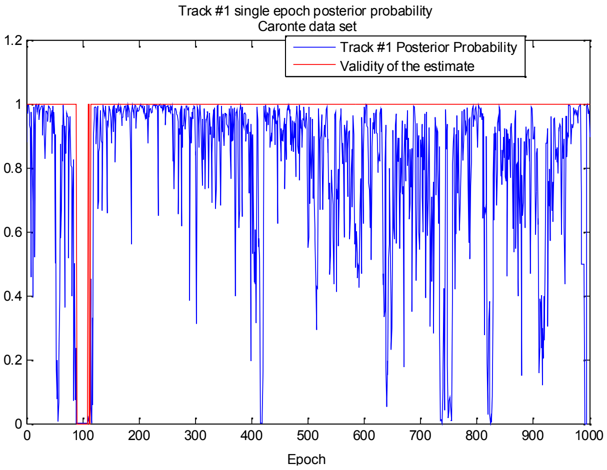

Figure 8. Posterior probability of the hypothesis corresponding to the true track based on single epoch observations.

In Figure 8 an excerpt of 1000 epochs (sampling interval of 1 sec.), corresponding to about the first 25 km of travelled distance, the posterior probability of the hypothesis corresponding to the true track (actually track #1), based on single epoch residuals, given by Eq. (40) is reported, together with the flag indicating the validity of the computed data.

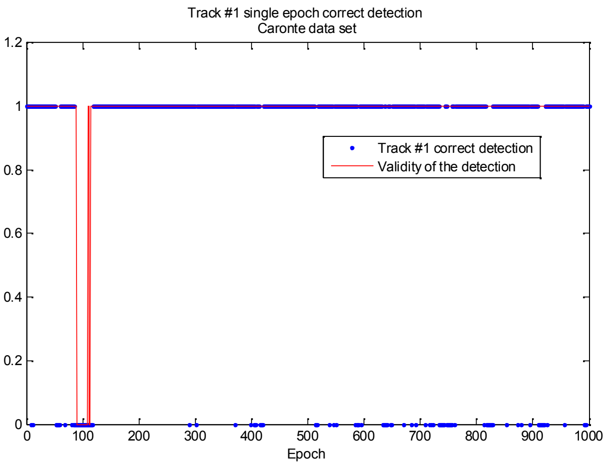

Figure 9. Correct detection of the hypothesis corresponding to the true track.

In Figure 9 the event corresponding to the correct track detection is also reported.

The experimental track error probability for the inter-track offset of 2 m. is about 0.15. This result is in good accordance with the value obtained from Eq. (46). In fact, for M=2, Δb=2 m, $\|\boldsymbol{\Gamma}_i \mathbf{b}_0\| / \|\mathbf{b}_0\| = 0.75$ and $\sigma_v = 0.75m$, the track error probability equals 0.158.

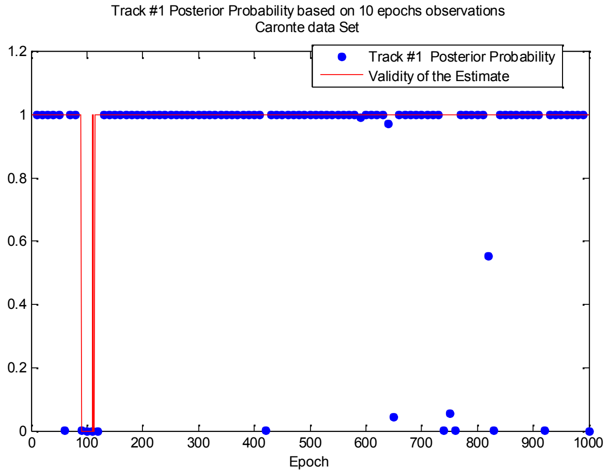

Figure 10. Posterior probability of the hypothesis corresponding to the true track based on 10 epochs observations.

In Figure 10 the posterior track probability based on 10 observations is also reported. Although at least 10 times more epochs should be employed to meet the required track error probability, statistical relevance of the reported results motivated the selection of a smaller number of epochs to verify the applicability of Eq. (50). The reported results evidenced that, in presence of signal degradations like those due to multipath, the errors are not statistically independent. Instead some form of clustering is present. The temporal correlation of the decisions (and consequently of the errors) may reduce the gain obtained by temporal integration, especially when a small number of epochs is employed.

VII. CONCLUSIONS

This paper has presented a novel solution to allow the discrimination of the track where the train is located, as a contribution for the adoption of GNSS on the ERTMS-ETCS train control system. As confirmed by the experimental activity, the joint use of a track database and GNSS measurements allow to discriminate the current train track.
To achieve track error probabilities compatible with SIL 4 operational requirements, temporal integration has to be performed when pseudoranges extracted from code tracking measurements are employed. Moreover, considering that track detector performance is driven by the ratio between the track offset and the receiver equivalent noise, some kind of augmentation (e.g. WAAS, EGNOS) has to be adopted to reduce the impact of ephemerides errors, and ionospheric and tropospheric incremental delays.

Since, based on Eq. (50), $\left\|\mathbf{\Gamma}_i \mathbf{b}_0\right\| / \left\|\mathbf{b}_0\right\|$ increases with the square root of the number of epochs employed in the decision, achievement of fast track discrimination requires a consistent reduction of the receiver equivalent noise, as the one achievable, for instance, by resorting to carrier phase tracking. On the other hand, the alternative solution based on the adoption of RTK mode requires a larger telecommunications bandwidth and a denser augmentation network, compared to the one actually deployed by the EGNOS system

APPENDIX A. TRACK ERROR PROBABILITY

Since the PVT estimation procedure operates on a linearized system, in order to compute the statistics of $\boldsymbol{\zeta}_{H_k}$ conditioned to the Hypothesis H_i, let us denote with $\hat{s}_i^{nf}$ the estimate of the train mileage for the i-th track in absence of receiver noise and multipath (noise-free case), under the condition that the i-th hypothesis is true. In addition let us denote with $\mathbf{b}_{i,k}$ the offset of the k-th track with respect the i-th one.

Using $\hat{s}_i^{nf}$ as initial point for the mileage estimation for the k-th hypothesis, with reference to Fig.2, the difference between the geometrical distance r_k^p between the p-th satellite and the point lying on the k-th track with mileage $\hat{s}_i^{nf}$, can be written in terms of the analogous quantity r_i^p of the i-th track, as follows

$$r_k^p \mathbf{e}_k^p = \left\langle \mathbf{b}_{k,i} + r_i^p \mathbf{e}_i^p, \mathbf{e}_k^p \right\rangle \mathbf{e}_k^p = \left\langle \mathbf{b}_{k,i}, \mathbf{e}_k^p \right\rangle \mathbf{e}_k^p + r_i^p \left\langle \mathbf{e}_i^p, \mathbf{e}_k^p \right\rangle \mathbf{e}_k^p \quad (52)$$

so that for their difference we have

$$\begin{aligned}\Delta r_{k,i}^p &= r_k^p - r_i^p = \\ &= r_i^p \left[\left\langle \mathbf{e}_i^p, \mathbf{e}_k^p \right\rangle - 1 \right] + \left\langle \mathbf{b}_{k,i}, \mathbf{e}_k^p \right\rangle,\end{aligned} \quad (53)$$

where $\mathbf{e}_k^p$ and $\mathbf{e}_i^p$ are the unit vectors corresponding to the lines-of-sights from the p-th satellite and the receiver lying on the i-th track and on the k-th track respectively.

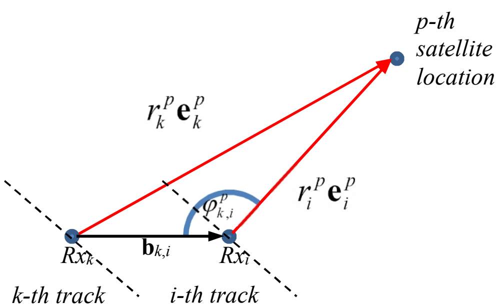

Figure 11. Receivers geometry

On the other hand, with reference to Figure 11, considering that:

$$r_k^p = r_i^p \sqrt{1 + \left(\frac{b_{k,i}}{r_i^p}\right)^2 - 2\frac{b_{k,i}}{r_i^p}\cos\left(\varphi_{k,i}^p\right)}\ , \quad (54)$$

and that for $|b_{k,i}|< 20$ m, for the GPS constellation we have

$$\left|\frac{b_{k,i}}{r_i^p}\right| < 10^{-6}, \quad (55)$$

the Taylor's expansion

$$\sqrt{1-\varepsilon} \cong 1 - \frac{\varepsilon}{2} \quad (56)$$

can be applied, so that for the single difference of the pseudoranges of the p-th satellite the following approximation holds

$$\Delta r_{k,i}^p \cong -b_{l,i}\cos\left(\varphi_{k,i}^p\right) + \frac{1}{2}\frac{b_{k,i}^2}{r_i^p} \cong -b_{l,i}\cos\left(\varphi_{k,i}^p\right). \quad (57)$$

Observing that

$$\left\langle \mathbf{b}_{k,i}, \mathbf{e}_i^p \right\rangle = -b_{k,i}\cos\left(\varphi_{k,i}^p\right) \quad (58)$$

we can finally write

$$\Delta \mathbf{r}_{k,i} = \mathbf{P}_i \mathbf{b}_{k,i}\,. \quad (59)$$

Therefore denoting with $\hat{z}_{H_k/H_i}$ the output of the k-th estimator when the true hypothesis is the i-th one, we have

$$\hat{z}_{H_k/H_i} = \hat{z}_{H_i} + \mathbf{K}\mathbf{P}_i \mathbf{b}_{k,i}\,. \quad (60)$$

Therefore it follows that

$$E\left\{\hat{\mathbf{v}}_{H_k} / H_i\right\} = \left(\mathbf{I} - \mathbf{H}\mathbf{K}\right)\mathbf{P}_i \mathbf{b}_{k,i}\,. \quad (61)$$

Similarly, we have

$$\boldsymbol{\zeta}_{H_k/H_i} = \boldsymbol{\zeta}_{H_i} + \mathbf{C}_{\mathbf{v}}(\mathbf{I} - \mathbf{H}\mathbf{K})\mathbf{P}_i \mathbf{b}_{k,i}\,. \quad (62)$$

For sake of compactness of notation let us pose

$$\mathbf{\Gamma}_i = \mathbf{C}_{\mathbf{v}}(\mathbf{I} - \mathbf{H}\mathbf{K})\mathbf{P}_i\,. \quad (63)$$

Then, we observe that the magnitude of $\boldsymbol{\zeta}_{H_k}$ will exceed the magnitude of $\boldsymbol{\zeta}_{H_k/H_i}$ as soon as the magnitude of the projection of $\boldsymbol{\zeta}_{H_k}$ into the direction of $\mathbf{\Gamma}_i \mathbf{b}_{k,i}$ will be greater than the half of the magnitude of $\mathbf{\Gamma}_i \mathbf{b}_{k,i}$ and its sign will be such that it will point in the opposite direction of $\mathbf{\Gamma}_i \mathbf{b}_{k,i}$. Considering that $\boldsymbol{\zeta}_{H_k}$ is a zero mean Gaussian variable with independent components with unitary variance, i.e.,

$$\boldsymbol{\zeta}_{H_i} \sim \mathcal{N}(0, \mathbf{I}) \quad (64)$$

the projection of $\boldsymbol{\zeta}_{H_k}$ into the direction of $\mathbf{\Gamma}_i \mathbf{b}_{k,i}$ will be a zero mean Gaussian random variable with unitary variance too.

In presence of multiple hypotheses, an error event is generated each time the lower threshold (i.e., the one associated to the adjacent track) is exceeded. Therefore the conditional probability of selecting one of the other tracks when the i-th track is the true one, given by Eq. (43) immediately follows.

To evaluate the track error probability increase due to undetected satellite faults and/or incremental ionospheric and tropospheric delays not fully compensated by the augmentation system, let us denote with $\Delta\xi_p$ the error affecting the *p*-th pseudorange due to the cited error sources. In this case the estimate $\hat{z}_{H_i}$ will be affected by the additional error $\mathbf{K}\Delta\xi$ so that:

$$E\left\{\hat{\mathbf{v}}_{H_i} / H_i\right\} = \left(\mathbf{I}-\mathbf{HK}\right)\Delta\xi\,, \qquad (65)$$

and

$$\zeta_{H_i} \sim \mathcal{N}\left(\mathbf{C}_{\mathbf{v}}\left(\mathbf{I}-\mathbf{HK}\right)\Delta\xi, \mathbf{I}\right) \qquad (66)$$

On the other hand, we have

$$\begin{aligned}\zeta_{H_k/H_i} &= \zeta_{H_i} + \mathbf{C}_{\mathbf{v}}(\mathbf{I}-\mathbf{HK})\mathbf{P}_i\mathbf{b}_{k,i} + \\ &+\mathbf{C}_{\mathbf{v}}(\mathbf{H}^{(i)}\mathbf{K}^{(i)} - \mathbf{H}^{(k)}\mathbf{K}^{(k)})\Delta\xi\,. \end{aligned} \qquad (67)$$

where the *i* and *k* superscripts have been introduced to remark that their values may be potentially different, being referred to different initial point for Taylor's expansion.

Thus denoting with $\mathbf{\Psi}^{(i,k)}$ the quantity

$$\mathbf{\Psi}^{(i,k)} = \mathbf{C}_{\mathbf{v}}(\mathbf{H}^{(i)}\mathbf{K}^{(i)} - \mathbf{H}^{(k)}\mathbf{K}^{(k)})\,, \qquad (68)$$

the conditional probability of selecting one of the other tracks when the i-th track is the true one, is

$$P_{e_i} = \begin{cases} \dfrac{1}{2} erfc\left\{\dfrac{\left\|\mathbf{\Gamma}_i\mathbf{b}_{2,1} + \mathbf{\Psi}^{(1,2)}\Delta\xi\right\|}{2\sqrt{2}}\right\} & i=1 \\ \dfrac{1}{2}\sum\limits_{\substack{k=i-1\\k\neq i}}^{i+1} erfc\left\{\dfrac{\left\|\mathbf{\Gamma}_i\mathbf{b}_{\mathrm{k,i}}\mathbf{\Psi}^{(i,\mathrm{k})}\Delta\xi\right\|}{2\sqrt{2}}\right\} & 1<i<M\,. \\ \dfrac{1}{2} erfc\left\{\dfrac{\left\|\mathbf{\Gamma}_i\mathbf{b}_{M-1,M} + \mathbf{\Psi}^{(\mathrm{M,M-1})}\Delta\xi\right\|}{2\sqrt{2}}\right\} & i=M \end{cases} \qquad (69)$$

REFERENCES

[1] Filip, A., Beugin, J., Marais, J. "Safety Concept of Railway Signalling Based on Galileo Safety-of-Life Service," COMPRAIL, Toledo, Spain, Sept 15-17, 2008, pp. 103-112.

[2] A. Neri, A. Filip, F. Rispoli, and A.M. Vegni, "An Analytical Evaluation for Hazardous Failure Rate in a Satellite-based Train Positioning System with reference to the ERTMS Train Control Systems," in Proc. of ION GNSS 2012, September 17-21, 2012, Nashville, TN, USA.

[3] Filip, A., Neri, A. Rispoli, F. "GNSS for railway signalling and train control: migration from aviation risk to hazard rate and safety integrity level," EUROPEAN Transport Research Review (manuscript submitted on June 10th, 2012).

[4] Filip, A. "Dependability Assessment of Satellite Based Augmentation System for Signalling and Train Control," International Heavy Haul Association Conference (IHHA 2011), Calgary, Canada, 19-22 June 2011.

[5] Rispoli F., Filip, A. ; Castorina, M. ; Di Mambro, G. ; Neri, A. ; Senesi, F., "Recent progress in application of GNSS and advanced communications for railway signaling", RADIOELEKTRONIKA, 2013 23rd International Conference, Pardubice, 16-17 April 201, Page(s):13 – 22, ISBN: 978-1-4673-5516-2, D.O.I. 10.1109/RadioElek.2013.6530882.

[6] Galileo Integrity Concept, ESA document ESA-DEUI-NG-TN/01331, 2005.

[7] S. Pullen, T., Walter, and P. Enge, "SBAS and GBAS Integrity for Non-Aviation Users: Moving Away from Specific Risk," Intl. Tech. Meeting of the Institute of Navigation, San Diego, CA, USA, pp.533-543, 2011.

[8] Van Trees, *Detection, Estimation, and Modulation Theory*, Part III, John Wiley & Sons, 2001.